

1 **What controls the thickness of continental crust in the Archean?**

2 **Vuong V. Mai¹, and Jun Korenaga¹**

3 *¹Department of Earth and Planetary Science, Yale University, PO Box 208109, New Haven,
4 Connecticut 06520-8109, USA. Email address: jun.korenaga@yale.edu*

5 **ABSTRACT**

6 Exposed continents are one of Earth's major characteristics. Recent studies on ancient
7 ocean volume and exposed landmasses suggest, however, that the early Earth was possibly a
8 water world where any significant landmass was unlikely to have risen above sea level. In the
9 modern Earth, the thickness of continental crust seems to be controlled by sea level and the
10 buoyancy of continental crust. Simply applying this concept to the Archean would not explain
11 the absence of exposed continents, and we suggest that a third element that is currently
12 insignificant was important during the early Earth: the strength of continental upper crust. Based
13 on pressure imbalance expected at continent-ocean boundaries, we quantify the conditions under
14 which rock strength controls the thickness of continental crust. With the level of radiogenic heat
15 production expected for the early Earth, continents may have been too weak to have maintained
16 their thickness against a deep ocean.

17

18 **INTRODUCTION**

19 Earth is covered by two different kinds of crust, oceanic and continental crust. The
20 normal oceanic crust is ~7 km thick (White et al., 1992), whereas the continental crust is ~40 km
21 thick on average (Christensen & Mooney, 1995). The thickness of oceanic crust is a simple
22 function of mantle potential temperature beneath mid-ocean ridges (McKenzie & Bickle, 1988);
23 a hotter mantle melts more, resulting in thicker oceanic crust. For the thickness of continental

24 crust, we do not expect such a genetic relationship with the state of the present-day mantle,
25 because the formation and evolution of continental crust are more complex, involving a variety
26 of tectonic processes over a timescale of billions of years. Instead, as suggested by Hess (1962),
27 the long-term thickness of continental crust may be regulated by a combination of isostasy and
28 sea level. Because the continental crust is less dense than the oceanic crust, isostasy allows the
29 former to be thicker than the latter. As the continental crust thickens, its surface eventually
30 exceeds the sea level, above which erosion becomes important. In the hypothesis of Hess (1962),
31 therefore, the thickness of continental crust is controlled by the ocean volume; a deeper ocean
32 allow the existence of thicker continental crust. This effect of ocean on continental height is well
33 understood in geology. The mean height of continents with respect to the sea level, known as the
34 continental freeboard (Wise, 1974), has been close to zero at least back to two billion years ago
35 (Korenaga et al., 2017).

36 Recent geochemical studies exploring the emergence of continents (Bindeman et al.,
37 2018; Johnson & Wing, 2020) have raised the possibility that most of the Archean was a water
38 world. A study on deep water cycle has also suggested that the Archean ocean could have been
39 more voluminous, with its surface reaching 4-6 km above mid-ocean ridges (Korenaga et al.,
40 2017). If the thickness of continents is regulated only by isostasy and sea level, however,
41 exposed continental crust seems inevitable even with a deep ocean. This is especially so because
42 the mass of continents is likely to have reached the present-day level in the early Earth
43 (Korenaga, 2018). Even with more gradual continental growth, continents can still grow to sea
44 level through thickening by orogeny.

45 In this study, we investigate the possibility that, in addition to sea level and isostasy, the
46 thickness of continental crust is also regulated by the strength of crustal rocks. Although it has

47 already been suggested that the Archean crust is too weak to have supported high mountains
48 (Rey & Coltice, 2008), previous studies have been limited to topographic variations *within*
49 continents. Here we consider the integrity of continents at a greater spatial scale, that is, with
50 respect to adjacent ocean basins. Our results suggest that, whereas strength does not seem to be a
51 limiting factor today, ductile flow could have been more important in the Archean.

52 In what follows, we first estimate differential stresses applied on the continental crust by
53 performing isostatic calculations. We also estimate temperature in the upper crust by calculating
54 the geotherm for both the modern and Archean Earth. As the concentration of heat-producing
55 elements in the Archean continental crust is still debated, we compare three cases: no secular
56 change in crustal composition (Guo & Korenaga, 2020), 75% less heat production (Condie,
57 1993), and 50% less heat production (Ptáček et al., 2020). From these stress and temperature
58 conditions, we evaluate the representative deformation rate of continental upper crust at the
59 present and in the Archean. Finally, we discuss how the Archean continental height might have
60 been controlled and what this implies for the early Earth landscape.

61

62 **MODEL SETTING**

63 The topography of continental crust and its overall thickness are controlled by different
64 mechanisms. The former is supported by variations in crustal thickness, for which the strength of
65 lower crust is important (e.g., Rey & Coltice, 2008). Higher radiogenic heat production and
66 higher mantle temperatures in the Archean could have weakened and even melted the lower crust
67 (Galer & Mezger, 1998), thereby limiting the surface relief. We expect a different mechanism to
68 control the average thickness of continents (cf. England & Molnar, 1997). At the boundary of
69 continental and oceanic domains, the horizontal flow of continental lower crust would be limited

70 by the surrounding oceanic lithosphere, leaving the continental upper crust to control the average
71 crustal thickness (Fig. 1). As the top portion of continental crust is bounded only by ocean, its
72 ability to support its own weight should determine the continental height. The strength of
73 continental upper crust is also better constrained by geological observations. The strength of
74 continental lower crust depends on its water content, lithology, and the depth distribution of
75 radiogenic heating (Burov & Diament, 1995), all of which are poorly constrained in deep time.
76 In contrast, the silica content of the continental upper crust is likely to have stayed relatively
77 constant through Earth history (Keller & Harrison, 2020). Crustal thickness may also be
78 regulated by delamination as thickened crust could stabilize garnet in the lower crust, but
79 delamination is not dynamically feasible under most conditions (Mondal & Korenaga, 2018).

80 In our model, pressure difference at the continent-ocean interface drives crustal flow, the
81 rate of which is controlled by the rheology of continental upper crust. A temperature profile
82 through the continental crust is calculated with the secular evolution of radiogenic heat
83 production and mantle potential temperature (see Supplementary Materials (SM) for details). The
84 flow law for the upper crust is based on our reanalysis of published deformation experiments on
85 quartz aggregates. When discussing the strength of crust or mantle, it is customary to calculate
86 yield stress for an assumed strain rate. In our model setting, however, stress driving deformation
87 is predetermined by the aforementioned pressure difference, so instead of yield stress, we
88 calculate strain rates corresponding to the pressure difference.

89 **Pressure Difference Between Continental and Oceanic Domains**

90 As the continental upper crust is denser than the surrounding seawater, the pressure
91 difference at the continent-ocean boundary drives the horizontal flow of continental crust into the
92 ocean (Fig. 1); this pressure difference exists at both passive and active margins. As the oceanic

93 lithosphere is denser than the continental crust, the pressure difference is reversed at greater
94 depths, and the continental lower crust is supported by the surrounding oceanic lithosphere.
95 Therefore, the overall thickness of continental crust is contingent on the free-flowing continental
96 upper crust. In our model, the compensation depth is taken to be at the base of continental
97 lithospheric mantle (Fig. 1), and the corresponding isostatic balance is given by:

$$98 \quad h_{cc}\rho_{cc} + h_{cm}\rho_{cm} = h_w\rho_w + h_{oc}\rho_{oc} + h_{om}\rho_{om} + h_m\rho_m, \quad (1)$$

99 where h and ρ denote thickness and density, respectively, and subscripts “cc”, “cm”, “w”, “oc”,
100 “om”, and “m” refer to continental crust, continental lithospheric mantle, water, oceanic crust,
101 oceanic lithospheric mantle, and asthenospheric mantle, respectively. Here the continental
102 structure is compared with the oceanic structure at the mid-ocean ridge, to provide a minimum
103 ocean depth at the continent-ocean boundary. More realistic cases with older seafloor are
104 considered in the discussion section. Our isostasy model is built on the continental freeboard
105 model of Korenaga et al. (2017), in which the thicknesses and densities of different layers and
106 their temporal evolution are estimated from a range of geological and geophysical observations
107 as well as theoretical considerations (see SM for a summary of key model parameters). In this
108 study, we vary the thickness of continental crust as a free parameter, and to provide a
109 conservative estimate on pressure difference, the top of continental crust is assumed to be at or
110 below sea level (Fig. 1).

111 **Strength of Upper Continental Crust**

112 The rheology of continental upper crust is usually considered to be controlled by that of
113 wet quartz aggregates (Kohlstedt et al., 1995; Bürgmann & Dresen, 2008). However, several
114 different flow laws have been published (e.g., Luan & Paterson, 1992; Gleason & Tullis, 1995;
115 Rutter & Brodie, 2004a,b; Fukuda et al., 2018), and predicted crustal strength varies substantially

116 with the choice of quartz flow law. Because crustal strength plays a central role in our analysis,
117 we have critically examined major deformation data on quartz aggregates, using the nonlinear
118 inversion method developed by Korenaga & Karato (2008) and amended by Mullet et al. (2015)
119 (see SM for details). We focus on ductile deformation because the available pressure difference
120 at the continent-ocean boundary does not exceed the brittle strength of rocks, assuming a friction
121 coefficient of 0.8 (Byerlee, 1978).

122 Our reanalysis shows that, as opposed to what Fukuda et al. (2018) suggested, there is
123 little experimental support for grain boundary sliding being the dominant deformation
124 mechanism of quartz aggregates. A combination of diffusion and dislocation creep is shown to
125 be sufficient to explain the published quartz deformation data, with dislocation creep being most
126 relevant under geological conditions. Our reanalysis further suggests that the deformation data of
127 Gleason & Tullis (1995) provide statistically the most reliable flow law. In this study, therefore,
128 we use the flow law derived from their data using our inversion.

129

130 **RESULTS**

131 Strain-rate profiles expected at the edges of continental crust were calculated for crustal
132 thicknesses between 35-60 km under present-day and Archean conditions. Representative
133 calculations are shown in Fig. 2 for a thickness of 40 km. The present-day strain rate does not
134 exceed the geological deformation rate of 10^{-15} s^{-1} (corresponding to the deformation time scale
135 of ~ 30 Myr for 100% strain) even at greater depths. In contrast, the Archean crust reaches the
136 geologic deformation rate at relatively shallow depths, suggesting that the continental upper crust
137 was capable of significant flow in the Archean, possibly limiting the continental height.

138 We focus on the strain rate at the base of the ocean (Fig. 3), because it is the highest
139 strain rate achievable in the upper crust adjacent to the ocean. The strain rate continues to
140 increase below the base of the ocean, but it is unlikely to be realized because the crust is bounded
141 by oceanic lithosphere at those depths. The strain rate calculated under present-day conditions is
142 much smaller than the geological strain rate of 10^{-15} s^{-1} for an almost entire range of crustal
143 thickness considered. For the early Archean, on the other hand, the relative buoyancy between
144 the continental and oceanic domains would place mid-ocean ridges at $\sim 6 \text{ km}$ below sea level
145 (Korenaga et al., 2017; Rosas & Korenaga, 2021), for which the continental crust had to be > 50
146 km thick to reach sea level (Fig. 3). Such crustal thickness is sufficient to produce a geologically
147 significant strain rate. This secular change in crustal strength arises partly because the crustal
148 geotherm was hotter in the past due to higher radiogenic heat production and higher mantle
149 temperature (Fig. 2) and partly because a slightly deeper part of the upper crust becomes relevant
150 for a deeper ocean in the past (Fig. 3).

151

152 **DISCUSSION**

153 So far, we focused on crustal strain rates expected at the depth of mid-ocean ridges.
154 However, the depth of ocean basins at the continent-ocean interface can be greater because of
155 seafloor subsidence. Thus, at realistic continent-ocean boundaries where old seafloor is adjacent
156 to continents, we can expect higher crustal strain rates because strain rates generally increase
157 with depth (Fig. 2). For comparison, strain rates expected in the case of a seafloor subsidence of
158 3 km, which is observed for present-day seafloor older than $\sim 100 \text{ Ma}$, is also shown in Fig. 3
159 (dashed lines). Even with this consideration, crustal strain rates are much lower than the
160 geological deformation rate (10^{-15} s^{-1}) under present-day conditions. Thus, it is reasonable to

161 conclude that crustal strength does not play any role in controlling continental thickness at
162 present. Under Archean conditions, on the other hand, the geological deformation rate is reached
163 when crustal thickness is greater than ~45 km, and this suggests a difficulty of growing
164 continents to reach sea level when the oceans is deeper than ~5 km at mid-ocean ridges (Fig. 3).
165 The stability of the Archean continental crust can be increased by lowering crustal heat
166 production, and with only 50% heat production, the crust may be able to grow up to ~55 km (Fig.
167 3), allowing it to emerge above sea level even when the mid-ocean ridge is ~6 km deep.

168 A real continent-ocean boundary would not be as sharp as depicted in Fig. 1, and a more
169 gradual transition reduces pressure difference. With pressure difference halved, for example, the
170 predicted strain rate would be lowered by around one order of magnitude given the stress
171 dependence of crustal rheology. This difference is smaller than the uncertainties associated with
172 flow-law predictions, seafloor subsidence, or crustal heat production (Fig. 3). Another realistic
173 complication not captured by our model is the effect of a cold skin layer of the continental crust
174 adjacent to the ocean. Such a cold layer would deform in a brittle regime, with a yield strength
175 being ~56% of lithostatic pressure, assuming a friction coefficient of 0.8 and hydrostatic pore
176 fluid pressure. As our model geometry conforms to the homogeneous stress condition, for which
177 the Reuss average is appropriate (Karato, 2008), upper-crustal flow would still be controlled
178 primarily by the ductile strength of a weaker interior as long as the cold skin layer is relatively
179 thin (see SM).

180 When we aim to understand the early Earth landscape, the importance of a theoretical
181 approach becomes apparent because relevant geological data are scarce. Given the available
182 experimental constraints on the strength of continental upper crust, it seems difficult for
183 continents to emerge from a deep ocean expected for the early Archean, unless the crust is

184 depleted in heat-producing elements. At the same time, our results also suggest that continental
185 crust could easily be thickened up to ~40 km even in the Archean (Fig. 3), so exposed continents
186 are possible if the ocean was not so deep. Because the history of ocean volume is unlikely to be
187 monotonic (Miyazaki & Korenaga, 2022), the possibility of exposed land, which plays an
188 essential role in some major hypotheses for the origin of life (e.g., Deamer, 2019), could depend
189 critically on a subtle balance between the growth of ocean and continents (Korenaga, 2021).
190 Given an ocean depth, our model can predict the maximum crustal thickness, and this capability
191 will be vital in estimating the extent of exposed land in the early Earth.

192

193 **ACKNOWLEDGMENTS**

194 This study is supported by U. S. National Science Foundation EAR-1753916 as well as Karen L.
195 Von Damm '77 Undergraduate Research Fellowship in Earth and Planetary Sciences at Yale
196 University. We thank Editor Gerald Dickens, Jolante van Wijk, Laurent Montesi, and four
197 anonymous reviewers for constructive comments and suggestions.

198

199 **REFERENCES CITED**

200 Bindeman, I. N., Zakharov, D. O., Palandri, J., Greber, N. D., Dauphas, N., Retallack, G. J.,
201 Hofmann, A., Lackey, J. S., and Bekker, A., 2018, Rapid emergence of subaerial landmasses and
202 onset of a modern hydrologic cycle 2.5 billion years ago: *Nature*, v. 557, p. 545–548,
203 <https://doi.org/10.1038/s41586-018-0131-1>.

204 Bürgmann, R., and Dresen, G., 2008, Rheology of the lower crust and upper mantle: Evidence
205 from rock mechanics, geodesy, and field observations: *Annual Reviews of Earth and Planetary
206 Sciences*, v. 36, p. 531–567.

207 Burov, E. B., and Diament, M., 1995, The effective elastic thickness (T_e) of continental
208 lithosphere: What does it really mean? *Journal of Geophysical Research*, v. 100, p. 3905–3927.

209 Byerlee, J., 1978, Friction of rocks, *PAGEOPH*, v. 116, p. 615–626.

210

214 Christensen, N. I., and Mooney, W. D., 1995, Seismic velocity structure and composition of the
215 continental crust: A global view: *Journal of Geophysical Research: Solid Earth*, v. 100, p. 9761–
216 9788, <https://doi.org/10.1029/95jb00259>.

217

218 Condie, K. C., 1993, Chemical composition and evolution of the upper continental crust:
219 Contrasting results from surface samples and shales, *Chemical Geology*, v. 104, p.1-37.

220

221 Deamer, D. W., 2019, *Assembling Life: How Can Life Begin on Earth and Other Habitable
222 Planets?* Oxford University Press, New York.

223

224 England, P., and Molnar, P., 1997, Active deformation of Asia: From kinematics to dynamics:
225 *Science*, v. 278, p. 647-650.

226

227 Fukuda, J., Holyoke, C. W., and Kronenberg, A. K., 2018. Deformation of fine-Grained quartz
228 aggregates by mixed diffusion and dislocation Creep: *Journal of Geophysical Research: Solid
229 Earth*, v. 123, p. 4676–4696, <https://doi.org/10.1029/2017jb015133>.

230

231 Galer, S. J. G., and Mezger, K., 1998, Metamorphism, denudation and sea level in the Archean
232 and cooling of the Earth: *Precambrian Research*, v. 92, p. 389–412,
233 [https://doi.org/10.1016/s0301-9268\(98\)00083-7](https://doi.org/10.1016/s0301-9268(98)00083-7).

234

235 Gleason, G. C., and Tullis, J., 1995, A flow law for dislocation creep of quartz aggregates
236 determined with the molten salt cell: *Tectonophysics*, v. 247, p. 1–23,
237 [https://doi.org/10.1016/0040-1951\(95\)00011-b](https://doi.org/10.1016/0040-1951(95)00011-b).

238

239 Guo, M., and Korenaga, J., 2020, Argon constraints on the early growth of felsic continental
240 crust: *Science Advances*, v. 6, eaaz6234, <https://doi.org/10.1126/sciadv.aaz6234>.

241

242 Hess, H. H., 1962, History of ocean basins, *in* Engel, A. E. J., James, H. L., and Leonard, B. F.,
243 eds., *Petrologic Studies: A Volume in Honor of A. F. Buddington*: Geological Society of
244 America, p. 599–620, <https://doi.org/10.1130/petrologic.1962.599>.

245

246 Hirth, G., Teyssier, C., and Dunlap, W. J., 2001, An evaluation of quartzite flow laws based on
247 comparisons between experimentally and naturally deformed rocks, *International Journal of
248 Earth Sciences*, v. 90, p. 77-87.

249

250 Johnson, B. W., and Wing, B. A, 2020, Limited Archaean continental emergence reflected in an
251 early Archaean ^{18}O -enriched ocean: *Nature Geoscience*, v. 13, p. 243–248,
252 <https://doi.org/10.1038/s41561-020-0538-9>.

253

254 Karato, S.-I., 2008, *Deformation of Earth Materials: Introduction to the Rheology of the Solid
255 Earth*: Cambridge University Press, New York, 463 p.

256

257 Keller, C. B., and T. M. Harrison, 2020, Constraining crustal silica on ancient Earth, *Proceedings
258 of the National Academy of USA*, v. 117, p. 21101-21107.

259

260 Kohlstedt, D. L., Evans, B., and Mackwell, S. J., 1995, Strength of the lithosphere: Constraints
261 imposed by laboratory experiments: *Journal of Geophysical Research*, v. 100, p. 17587–17602.
262

263 Korenaga, J., and Karato, S.-I., 2008, A new analysis of experimental data on olivine rheology:
264 *Journal of Geophysical Research*, v. 113, B02403, <https://doi.org/10.1029/2007jb005100>.
265

266 Korenaga, J., Planavsky, N. J., and Evans, D. A. D., 2017, Global water cycle and the
267 coevolution of the Earth’s interior and surface environment: *Philosophical Transactions of the
268 Royal Society A: Mathematical, Physical and Engineering Sciences*, v. 375, 20150393,
269 <https://doi.org/10.1098/rsta.2015.0393>.
270

271 Korenaga, J., 2018, Crustal evolution and mantle dynamics through Earth history: *Philosophical
272 Transactions of the Royal Society A: Mathematical, Physical and Engineering Sciences*, v. 376,
273 20170408, <https://doi.org/10.1098/rsta.2017.0408>.
274

275 Korenaga, J., 2021, Was there land on the early Earth?: *Life*, v. 11, 1142,
276 <https://doi.org/10.3390/life1111142>.
277

278 Luan, F. C., and Paterson, M. S., 1992, Preparation and deformation of synthetic aggregates of
279 quartz: *Journal of Geophysical Research*, v. 97, p. 301–321, <https://doi.org/10.1029/91jb01748>.
280

281 McKenzie, D., and Bickle, M. J., 1988, The volume and composition of melt generated by
282 extension of the lithosphere: *Journal of Petrology*, v. 29, p. 625–679,
283 <https://doi.org/10.1093/petrology/29.3.625>.
284

285 Mondal, P., and Korenaga, J., 2018, A propagator matrix method for the Rayleigh-Taylor
286 instability of multiple layers: a case study on crustal delamination in the early Earth: *Geophys. J.
287 Int.* v. 212, p. 1890–1901, <https://doi.org/10.1093/gji/ggx513>.
288

289 Miyazaki, Y., and Korenaga, J., 2022, A wet heterogeneous mantle creates a habitable world in
290 the Hadean: *Nature*, v. 603, p. 86–90.
291

292 Mullet, B. G., Korenaga, J., and Karato, S.-I., 2015, Markov chain Monte Carlo inversion for the
293 rheology of olivine single crystals: *Journal of Geophysical Research: Solid Earth*, v. 120, p.
294 3142–3172, <https://doi.org/10.1002/2014jb011845>.
295

296 Ptáček, M. P., Dauphas, N., and Greber, N. D., 2020, Chemical evolution of the continental crust
297 from a data-driven inversion of terrigenous sediment compositions, *Earth and Planetary Science
298 Letters*, v. 539, p. 116090.
299

300 Rey, P. F., and Coltice, N., 2008, Neoarchean lithospheric strengthening and the coupling of
301 Earth’s geochemical reservoirs: *Geology*, v. 36, p. 635–638, <https://doi.org/10.1130/g25031a.1>.
302

303 Rosas, J. C., and Korenaga, J., 2021, Archaean seafloors shallowed with age due to radiogenic
304 heating in the mantle: *Nature Geoscience*, v. 14, p. 51–56, [https://doi.org/10.1038/s41561-020-00673-1](https://doi.org/10.1038/s41561-020-
305 00673-1).

306
307 Rutter, E. H., and Brodie, K. H., 2004a, Experimental grain size-sensitive flow of hot-pressed
308 Brazilian quartz aggregates: *Journal of Structural Geology*, v. 26, p. 2011–2023,
309 <https://doi.org/10.1016/j.jsg.2004.04.006>.
310
311 Rutter, E. H., and Brodie, K. H., 2004b, Experimental intracrystalline plastic flow in hot-pressed
312 synthetic quartzite prepared from Brazilian quartz crystals: *Journal of Structural Geology*, v. 26,
313 p. 259–270, [https://doi.org/10.1016/s0191-8141\(03\)00096-8](https://doi.org/10.1016/s0191-8141(03)00096-8).
314
315 White, R. S., McKenzie, D., and O’Nions, R. K., 1992, Oceanic crustal thickness from seismic
316 measurements and rare earth element inversions: *Journal of Geophysical Research*, v. 97, 19683–
317 19715, <https://doi.org/10.1029/92jb01749>.
318
319 Wise, D. U., 1974, Continental margins, freeboard and the volumes of continents and oceans
320 through time, in Burk, C. A., and Brake, C. L., eds., *The Geology of Continental Margins*:
321 Springer, p. 45–58, https://doi.org/10.1007/978-3-662-01141-6_4.
322

323

324

325

326 FIGURE CAPTIONS

327 **Figure 1.** Schematic drawing for compositional stratifications in the top few hundred kilometers
328 of Earth: (A) continental domain and (B) oceanic domain. Different layers have different
329 thicknesses and densities as indicated. These layers are drawn not to scale. Dotted lines indicate
330 expected crustal flow based on horizontal pressure imbalance and rock rheology. Dashed
331 rectangle denotes the main focus of our modeling (Fig. 2).

332 **Figure 2.** Modeling strain-rate profiles for present-day and Archean crust with a thickness of 40
333 km. (A) and (B) show predicted pressure differences as a function of depth for present-day and
334 Archean Earth, respectively. (C) shows present-day (blue) and Archean (red) geotherms, and (D)
335 shows the corresponding strain-rate profile (shading indicates interquartile range corresponding
336 to the uncertainty of quartz flow law). For comparison, the Archean geotherms with 75%

337 (orange) and 50% (green) heat production are shown in (C), and Archean strain-rate predictions
338 according to the original flow law of Gleason and Tullis (1995) (black dashed) and the field-
339 based flow law of Hirth et al. (2001) (black dotted; see SM for its uncertainty) are shown in (D).

340 **Figure 3.** (top) Depth of mid-ocean ridges (h_v) corresponding to continental thicknesses,
341 according to the freeboard model of Korenaga et al. (2017). (bottom) Crustal strain rate, as a
342 function of continental thicknesses, at the base of the ocean (e.g., at \sim 2.5 km depth at present in
343 Fig. 2D): present-day (blue) and Archean (red), with shading for interquartile range. Median
344 strain rates at depth of 3 km below the ridge depth are shown in dashed. Also shown are two
345 more Archean predictions, at depth of 3 km below ridge depth, with 75% (red dot-dashed) and
346 50% (red dotted) heat production.

347

348 ¹GSA Data Repository item 201Xxxx, Reanalysis of the deformation data of quartz aggregates
349 and the details of strain rate modeling, is available online at
350 www.geosociety.org/pubs/ft20XX.htm, or on request from editing@geosociety.org.

Figure 1

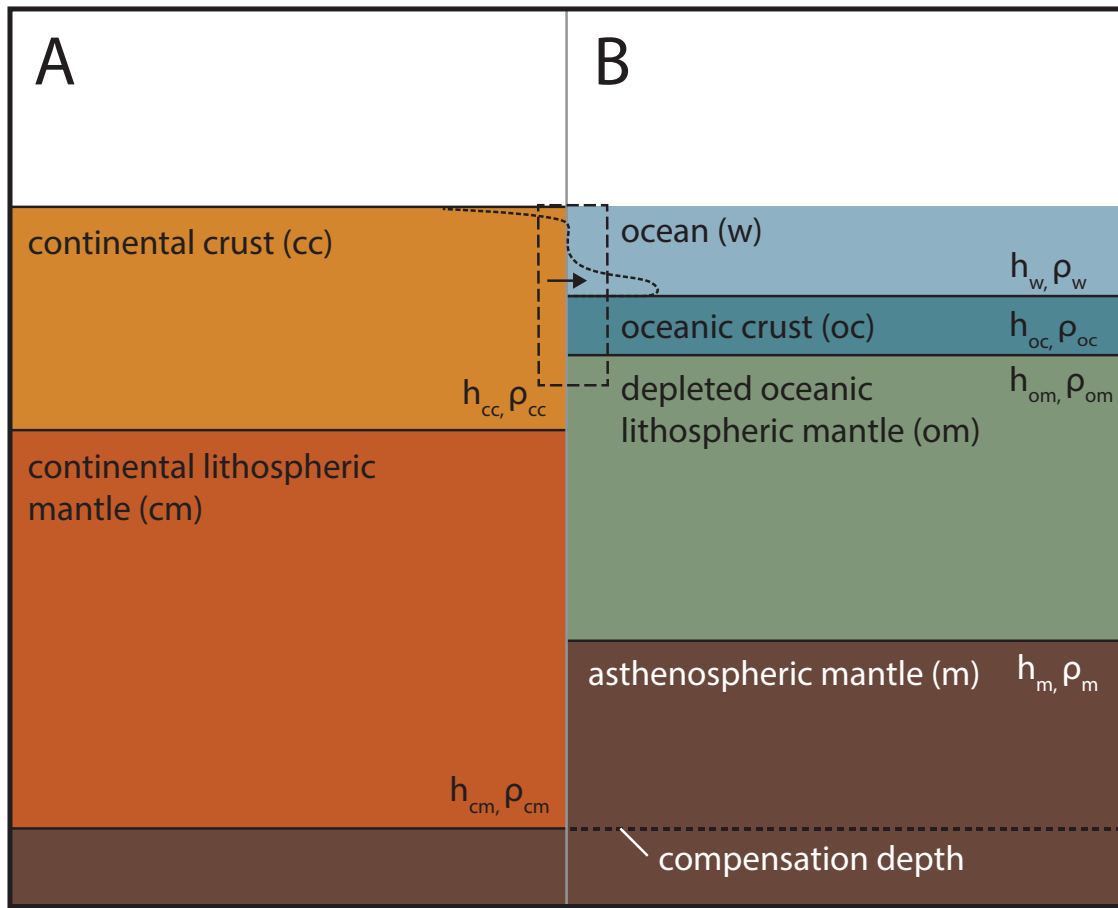
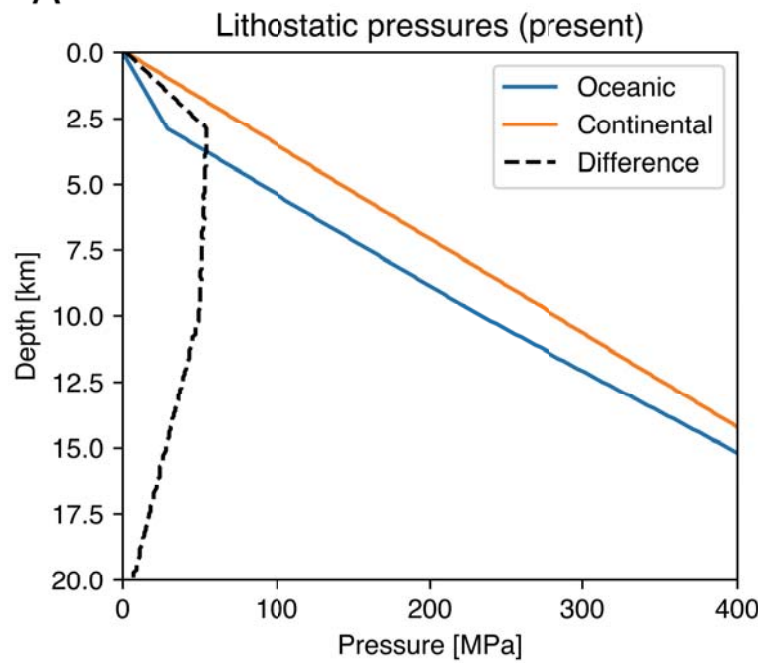


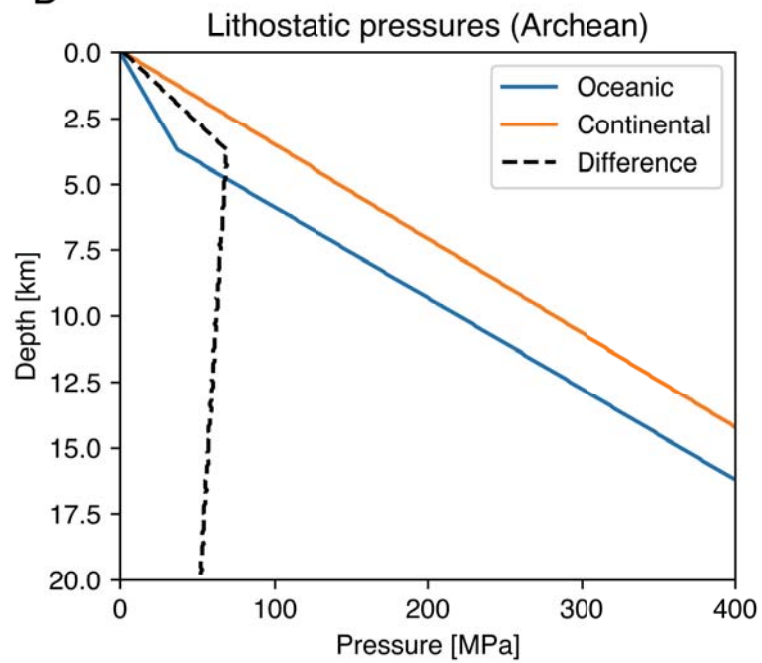
Figure 2

Continental thickness = 40.0 km

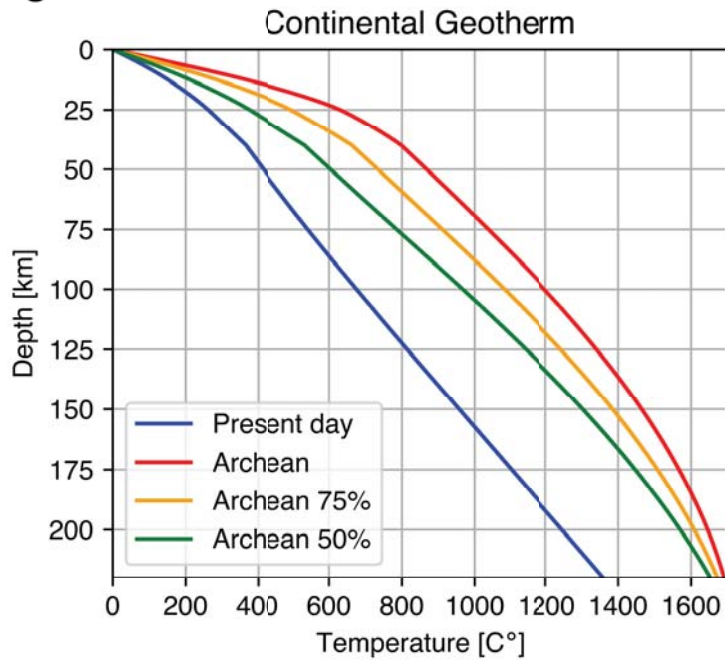
A



B



C



D

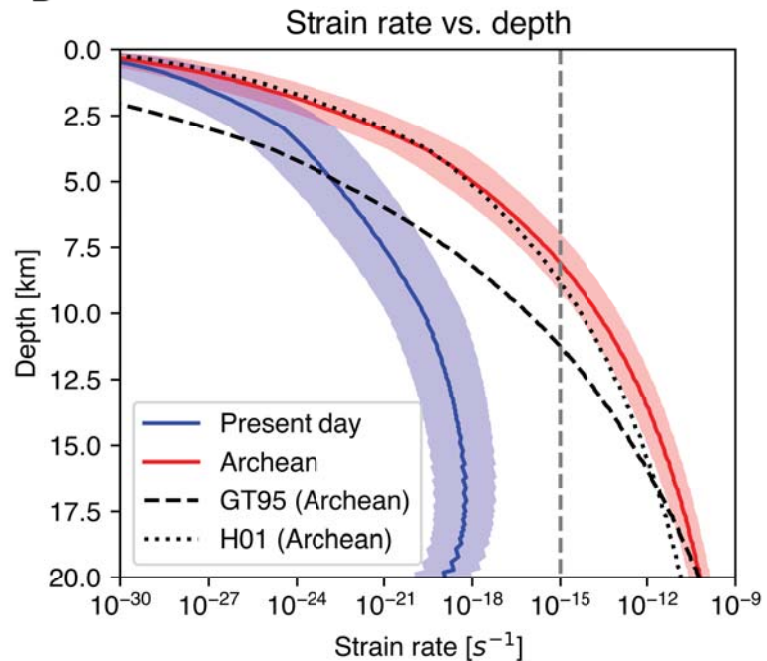


Figure 3

